Mechanical, Thermal, and Barrier Properties of PHBH/Cellulose Biocomposite Films Prepared by the Solution Casting Method

Junran Li,[a,b] Fen Yin,[a] Dongna Li,[a] Xiaojun Ma,[a,*] and Jiao Zhou [a]

A biocomposite film from bacterial polyester, poly(3- hydroxybutyrate-co-3-hydroxyhexanoate) (PHBH), and natural cellulose was developed by the solution casting method. The structure, the mechanical, thermal, and barrier properties (oxygen and water vapor), and the biodegradation of the PHBH/cellulose biocomposite films were studied. With an increase in cellulose content, the tensile strength of biocomposite films increased from 28.5 MPa to 45.9 MPa, an improvement of 351% compared with neat PHBH. The PHBH/cellulose biocomposite films exhibited improved thermal stability, with the maximum thermal decomposition temperature increased from 264 °C to 330 °C. More importantly, PHBH/cellulose biocomposite films possessed better barrier properties against oxygen, up to approximately 10 times more than neat PHBH. With cellulose content increased from 50 wt% to 90 wt%, the mass loss of composite films increased gradually and then decreased. This high performance biocomposite has potential to expand the use of cellulose from renewable bioresources and the practical application of PHBH-based biodegradable plastics instead of traditional petrochemical materials in the packaging field.

Keywords: Biocomposite; Cellulose; PHBH; Permeability; Mechanical properties; Thermal properties

*Contact information: a: College of Packaging & Printing Engineering, Tianjin University of Science & Technology, Tianjin 300222, China; b: Tianjin Bokelin Medical Packaging Technology Co., Ltd., Tianjin 300410, China; *Corresponding author: mxj75@tust.edu.cn*

INTRODUCTION

Recently, due to the widespread application of petroleum-based plastics, a series of environmental problems and a shortage of petroleum fuel have gradually developed (Hosoda *et al*. 2014). Therefore, eco-friendly biodegradable plastics have become the focus of attention. Polyhydroxyalkanoates (PHAs) are crystalline homopolymers produced by microbial fermentation and have good biodegradability and biocompatibility (Kynadi and Suchithra 2017). Poly (3-hydroxybutyrate-co-3-hydroxyhexanoate) (PHBH), a promising member of the PHA family, is a copolymer consisting of randomly arranged 3-hydroxybutyrate (3HB) and 3-hydroxyhexanoate (3HH) units (Zhou *et al*. 2015). They have numerous qualities that are superior to polyhydroxybutyrate (PHB), including low melting point and ductile properties. The amount of the 3HH fraction in PHBH strongly influences the properties of a polymer matrix, such as crystallinity, melting point, strength, and crystallization rate, all of which are considered as an optimal environmentally friendly packaging material. However, PHBH also has some disadvantages, such as a high price, low strength modulus, and poor thermal stability, which limit its extensive utilization (Xie *et al*. 2009).

In order to overcome the above weaknesses, great efforts have been made in research. Cellulose (obtained from cotton fiber, pulp, wood, *etc*.) has received much attention due to its strong mechanical properties and chemical reactivity. More importantly, cellulose is an inexpensive, biodegradable, and renewable resource, compared with synthetic polymers (Luo *et al*. 2017; Wang *et al*. 2018a). Meanwhile, the results show that cellulose obtained from natural fibers is widely utilized as a filler in biocomposites to improve their thermal stability, as well as their mechanical and barrier properties (Dong *et al*. 2010; Jie *et al*. 2016; Lin *et al*. 2016; Codou *et al*. 2017; Dasan *et al*. 2017). However, the dispersion of cellulose, due to poor compatibility between the relatively hydrophilic cellulose with the hydrophobic polymer matrix, results in inefficient compounding with most nonpolar thermoplastics (Hosoda *et al*. 2014). In some cases, the solution casting method could be an effective approach for overcoming this challenge (Malmir *et al*. 2017). Presently, there is little information available on the processing of PHBH/cellulose biocomposites.

Based on the above considerations, the objective of this study was to improve the compatibility between PHBH and natural cellulose *via* the solution casting method. A novel biocomposite was obtained. The effects of the mixing ratios between PHBH and cellulose on the micrographs, structures, and thermal and mechanical properties of the resulting copolymers were studied. The barrier properties of the biocomposites were also investigated experimentally and statistically.

EXPERIMENTAL

Materials

The PHBH containing 11 mol% 3HH (M_w = 6 × 10^5) was a gift from Japan Kaneka Co (Osaka, Japan). Cellulose (the cotton linter pulp) with a degree of polymerization of 475, an intrinsic viscosity of 8.25 MPa·s, and a whiteness of 79% was purchased from Qingdao Liyuan Dade International Trade Co., Ltd. Trifluoroacetic acid, analytical grade, was purchased from Tianjin Fuqi Chemical Co., Ltd.

Preparation of PHBH/Cellulose Composite Films

The following procedure has been typically used in the preparation of PHBH/cellulose biocomposite films. A total mass of 2 g of PHBH and cellulose were dispersed in trifluoroacetic acid solution, and the mixture was stirred at room temperature for 24 h and then allowed to stand 24 h to yield a clear solution. The solution was cast on a Teflon plate, and the obtained PHBH/cellulose biocomposite films were vacuum-dried at 60 °C for 48 h to remove residual acid solvents completely. The cellulose contents of the biocomposite films were 50 wt%, 60 wt%, 70 wt%, 80 wt%, and 90 wt%, named PC50, PC60, PC70, PC80, and PC90, respectively. Meanwhile, untreated PHBH and neat cellulose were used as controls.

Characterization

A scanning electron microscope (SEM) (JSM-6360LV, JEOL, Tokyo, Japan) with an acceleration voltage of 5 kV was used to analyze the fracture surface of the composite films. All the nanocomposite sheets were frozen in liquid nitrogen and then immediately snapped. The fracture surfaces of the sheets were sputtered with gold and then observed and photographed.

Fourier transform infrared spectroscopy (FT-IR, Nicolet-6700, Thermo Scientific, Waltham, MA, USA) was adopted to measure the samples and obtain IR spectra. The samples were tested by preparation of 1:300 KBr discs, with a scanning time of 16 s, resolution of 4 cm^{-1}, and scanning range of 400 cm^{-1} to 4000 cm^{-1}.

X-ray diffraction (XRD) of composite films was performed to test the crystallinity on a power X-ray diffractometer (D/max-2500, Rigaku, Tokyo, Japan) using Cu K α radiation (wavelength was 0.154 nm, powdered samples). The XRD analysis conditions were as follows: scanning range of 5° to 60°, scanning rate of 2° /min at 40 kV and 30 mA.

Mechanical properties of the samples were measured using an Instron Universal Testing Machine (Model 3369, Instron, Boston, MA, USA) according to ASTM D882-10 (2010). Smooth and uniform parts of cast film samples with the length of 175 mm, the width of 10mm, the thickness of 50 μm were selected. The machine was operated with an initial grip separation of 50 mm and a crosshead speed of 50 mm/min. Then, the tensile strength and elongation at break were measured. Five replicates were tested for each sample, and the average values are presented.

Thermogravimetric analysis (TGA) was conducted using a TG209 (Netzsch Instrument Co., Ltd., Germany) to determine the thermal stability of the samples. Approximately 5 mg of each sample was taken in a standard aluminum pan and heated from 0 °C to 450 °C at a heating rate of 10 °C/min in N_2 atmosphere (20 $mL \cdot min^{-1}$).

The water vapor transmission (WTR) of the composite films was estimated gravimetrically following the standard method of GB/T 1037-1988 (1988). Oxygen permeability of the composite films was evaluated using a gas permeability tester (GDP-C, Brügger, Bremen, Germany) at room temperature. For each sample, three replicates were performed and the average values were reported.

Samples were cut into 1 cm × 3 cm and buried in the ground 15 cm deep. The samples were taken out every three days and then washed with distilled water, dried, and weighed. The mass loss rate of the samples was calculated as an indicator of degradation performance of the biocomposites. The degradation performance was recorded to calculate the mass loss rate according to the following equation,

$$W = [(W_0 - W_1) / W_0] \times 100\% \quad (1)$$

where W, W_0, and W_1 are the mass loss rate (%), mass before film embedding (g), and mass after film removal (g), respectively.

RESULTS AND DISCUSSION

Morphological Characteristics

The cross-sectional micrographs of the PHBH/cellulose biocomposites are shown in Fig. 1. The cross-section of PHBH was tidy with a porous structure (Fig. 1(a)). Compared with neat PHBH, the tiny holes disappeared, and a lamellar structure appeared in PHBH/cellulose biocomposites with increasing cellulose content (Fig. 1(b) to (f)). When the cellulose content was from 50 to 70%, there were voids and holes in the cross-section of the samples (Fig. 1(b) to (d)), which can be ascribed to the poor interfacial bonding and the phase separation between PHBH and cellulose. Figures 1(e) and (f) show the obvious lamellar structure. The PC90 was more compact, which may be due to the strong interaction between PHBH and cellulose molecules in the composites. Moreover,

these composites showed some visible signs of fiber pull-out (Anderson *et al*. 2013), and the length of the pull-out fiber increased.

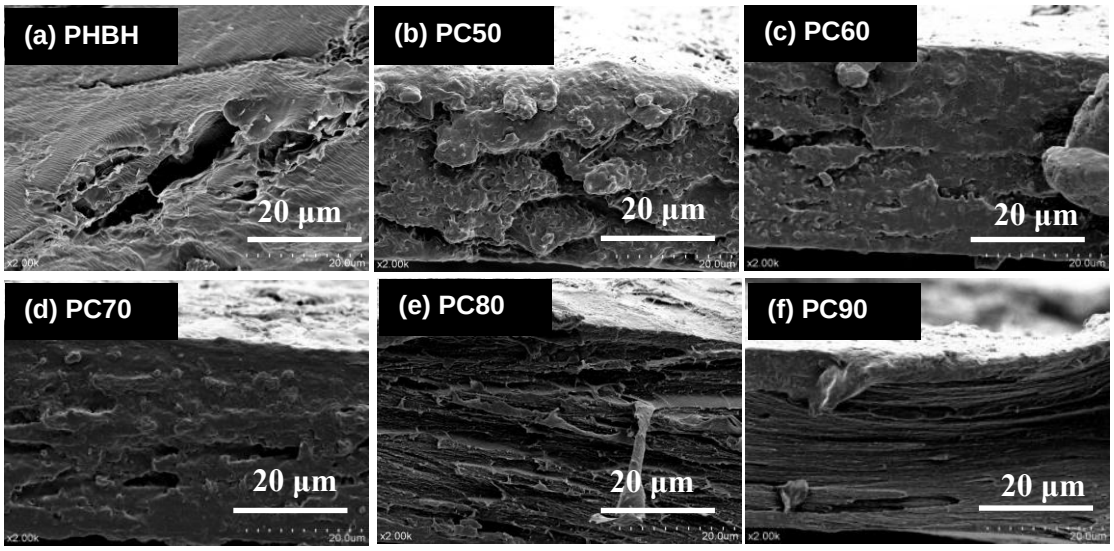

Fig. 1. Cross-section SEM images of PHBH/cellulose composites

XRD Analysis

The XRD curves of PHBH, cellulose, and the PHBH/cellulose composite films are illustrated in Fig. 2(a). The peaks of neat PHBH at 13.66°, 17.16°, 22.10°, 25.68°, and 31.42 could assigned to the (020), (110), (111), (031), and (002) planes. The peaks of cotton fiber at 15.12°, 16.22°, 22.82°, and 34.74° could correspond to the (101), (110), (002), and (004) planes of cellulose I (Vanitjinda *et al*. 2018). All of the above were the characteristic diffraction peaks of cellulose I. The regenerated cellulose showed a characteristic cellulose II reflection at 20.06°, which was assigned to the (110) plane. These results indicated that cellulose I was changed to cellulose II during cellulose dissolution (Nie *et al*. 2018).

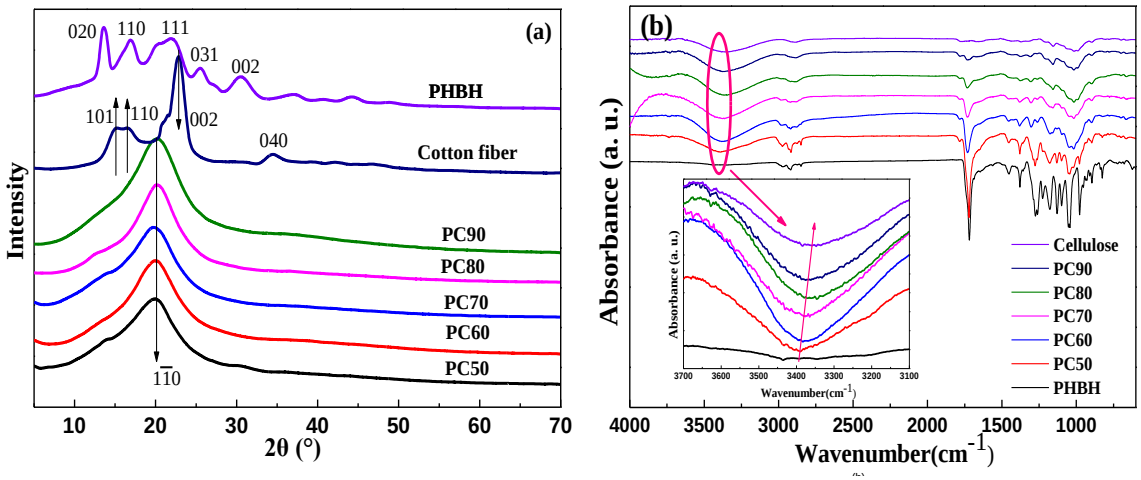

Fig. 2. XRD and FTIR curves of PHBH/cellulose composites: (a) XRD, (b) FTIR

When the cellulose content was increased from 50 wt% to 90 wt%, the position of the diffraction peaks of PHBH/cellulose composite films was close to that of the neat cellulose diffraction peak without the PHBH diffraction peak appearing. The intensity of each peak showed almost no obvious deviation, indicating that the addition of PHBH did not alter the crystalline form of the cellulose. Cellulose and composite materials showed a single broad band, which was related to the trifluoroacetic acid used for dissolving the component broke the H-bond network of cellulose, affected the regularity of polymer molecular arrangement, resulting in the destruction of crystalline region and the decrease of crystallinity. It may also be related to the addition of PHBH.

FTIR Analysis

Figure 2(b) shows the FTIR spectra of PHBH, cellulose, and PHBH/cellulose biocomposites. All the characteristic peaks of PHBH and cellulose appeared in the FTIR spectra for the composite films. It can be seen from the graph that, with increasing cellulose content, the peak intensity near 2974 cm^{-1}, representing C-H stretching vibration modes of PHBH alkyl, was gradually weakened, and the peak intensity near 2890 cm^{-1}, representing the C-H stretching vibration modes of cellulose, was strengthened gradually. Additionally, the bands at 2883 cm^{-1}, 1370 cm^{-1}, 1263 cm^{-1}, 1315 cm^{-1}, and 1041 cm^{-1}, representing stretching vibration of C-H, symmetric and asymmetric bending vibration of C-H, rocking vibration of C-H, and stretching vibration of C-O-C of cellulose, respectively, appeared and strengthened gradually (Adebajo and Frost 2004). It was obvious that the area of the O-H stretching band increased near 3389 cm^{-1} when the cellulose content increased from 50 to 90%. This is related to the intermolecular hydrogen bonds formed by cellulose and PHBH and the destruction of the crystalline structure of composite materials, which is consistent with the result of XRD. Meanwhile, with the cellulose content increasing, the O-H stretching band shifted to lower wavenumbers of the typical values of pure cellulose.

Mechanical Properties

The tensile strengths and Young's modulus (a) and elongations at break (b) of PHBH, cellulose, and the PHBH/cellulose composites are displayed in Fig. 3. With an increase of cellulose content, the tensile strength of PHBH/cellulose composite films increased, the Young's modulus decreases first and then increases, and the elongation at break of PHBH/cellulose composite films decreased. The tensile strength of composite film increased from 28.5 MPa to 45.9 MPa with the increase of cellulose content. The tensile strength of PC90 reached a maximum value of 45.9 MPa, a 351% improvement compared with that of neat PHBH film and a 44% improvement compared with that of neat regenerated cellulose film. The mechanical effect of cellulose on PHBH was remarkable. This result suggests that PHBH was well dispersed into the cellulose network, and the structure of cellulose macromolecules became dense. Moreover, there was a strong interface between the PHBH chain and cellulose, which allowed stress transfer between cellulose and PHBH, resulting in the tensile strength increasing. The Young's modulus of PC90 (1808 MPa) reaches a 223% improvement compared with that of neat PHBH film (559 MPa), is lower than that of cellulose. It can be seen that the cellulose content can promote the increase of Young's modulus, resulting in the mechanical properties increasing.

The elongation at break reached a maximum value of 28.5% at cellulose content of 50%, a 106% improvement compared with that of neat PHBH film and a 214%

improvement compared with that of neat cellulose film. This can be ascribed to the decrease of cellulose crystallinity. With the increase of cellulose content, the elongation at break of the composite films decreased from 28.5% to 15.4%, which may be due to the interaction between cellulose and PHBH, forming intermolecular hydrogen bonds. It was also related to the rigidity of cellulose molecules.

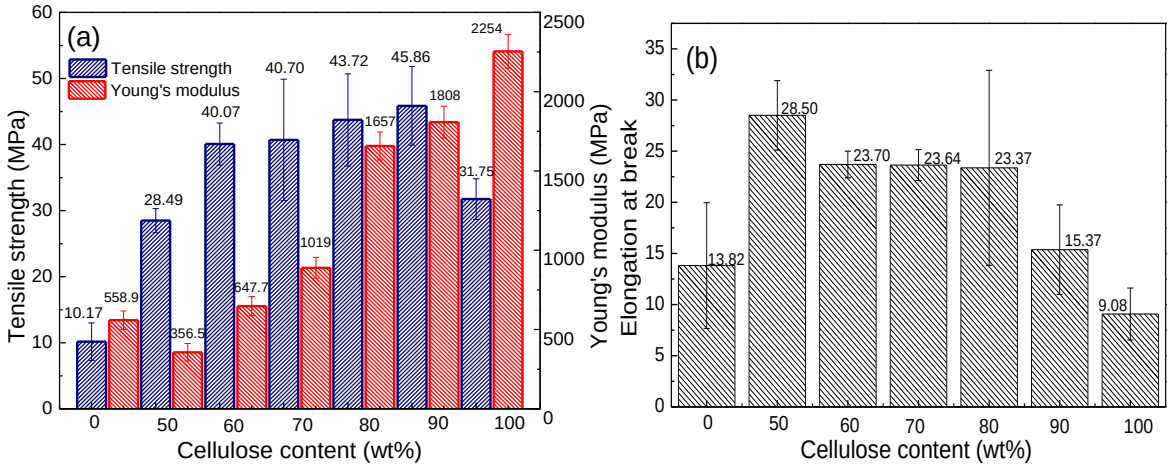

Fig. 3. Mechanical properties of PHBH/cellulose composites: (a) tensile strength, (b) elongation at break

Thermal Stability Analysis

Figure 4 shows typical TG curves of PHBH, cellulose, and PHBH/cellulose composite films. It is apparent that PHBH had good thermal degradation through a one-step process. The thermal stability of PHBH was as high as 225 °C with almost no mass loss. The TG curves of cellulose and PHBH/cellulose composite films exhibited stepwise degradation behaviors. The curves from room temperature to about 100 °C were relatively flat, and the mass loss can be ascribed to the evaporation of moisture. The mass loss from approximately 197 °C to 250 °C was the thermal decomposition of PHBH, and the mass loss near 295 °C to 395 °C was the decomposition of cellulose (Jiang and Hsieh 2013; Hosoda *et al*. 2014). It is found that the decomposition curve of cellulose mainly had two stages. The first stage occurs over the temperature range of 197 to 300 °C, which is due to the thermal degradation of cellulose in amorphous region and the destruction of crystalline region. The second stage occurs over the temperature range of 300 to 414 °C, which can be attributed to the final decomposition of cellulose.

Main thermal parameters are summarized in Table 1. With increasing cellulose content, the maximum thermal decomposition temperature (T_{max}) and the end decomposition temperature (T_{end}) of the composite films were increased. When the cellulose content was 90%, the first decomposition temperature (T_1) and T_{max} were higher than those of other samples, exhibiting excellent thermal stability. It was caused by the strong interaction between PHBH and cellulose. With the increase of cellulose content, the residue of samples also showed an increasing trend. This may be because the residue is mainly related to cellulose content. As can be seen from Table 1, the second decomposition temperature (T_2) and the end decomposition temperature (T_{end}) of the composites were lower than that of cellulose, which may be caused by the decreased crystallinity of the composites.

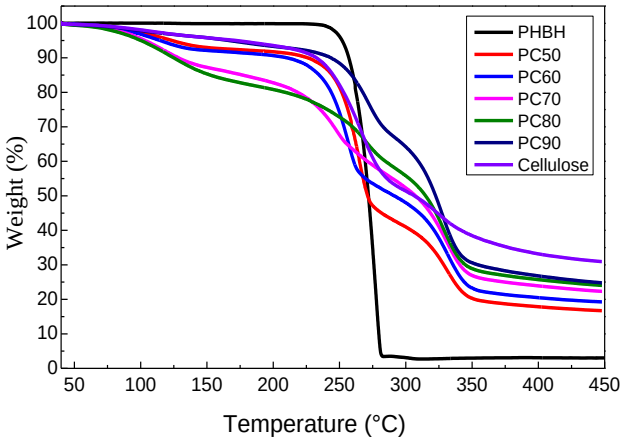

Fig. 4. TG curves of PHBH/cellulose composites

Table 1. Thermal Analysis Parameters of PHBH, Cellulose, and PHBH/cellulose Film

Samples	T_1 (°C)	T_2 (°C)	T_{end} (°C)	T_{max} (°C)	Residue (%)
PHBH	225	-	300	275	3
PC50	195	298	379	264	16
PC60	191	292	383	256	19
PC70	191	290	387	327	22
PC80	189	291	387	328	24
PC90	208	292	395	330	25
Cellulose	197	300	414	266	31

Barrier Properties

Water vapor and oxygen transmission rates of PHBH, cellulose, and PHBH/ cellulose composites were studied, and the results are presented in Fig. 5(a). As shown, the WTR of the composites gradually increased and the water vapor resistance gradually decreased with the increase of cellulose content. This can be attributed to the reduction of PHBH particles, such that the content of hydrophobic groups was lower and that of the hydrophilic groups was higher in the composite films. This resulted in more water vapor permeating the composite films (Lin *et al.* 2016). Because the PHBH was hydrophobic, its WTR was minimal, and its water vapor resistance was maximal. However, cellulose, containing a large number of hydroxyl groups, is hydrophilic, so its WTR was maximal, and its water vapor resistance was minimal. With decreased cellulose content, the decreased WVT of PHBH/cellulose composite films was due to the water-vapor-impermeable PHBH chains, which formed a tortuous path for the diffusion of water vapor through the polymer matrix (Shankar *et al*. 2017; Wang *et al.* 2018b).

As shown in Fig. 5(a), with the increase of cellulose content, the oxygen transmittance coefficient of the composite films first decreased and then increased, which is attributable to the gradual appearance of lamellar structure in the composite films. Furthermore, the lamellar structure tended to be dense. Simultaneously, the total amount of hydrogen bonds gradually increased, making the binding between macromolecules more compact. The oxygen barrier of PC80 and PC90 was better than that of neat cellulose film, which was due to the good compatibility between PHBH and cellulose macromolecules and the formed hydrogen bonds between macromolecules. The oxygen

barrier of PHBH film was the worst, which is attributable to the large number of pores on the surface of PHBH film and the loose structure of PHBH film.

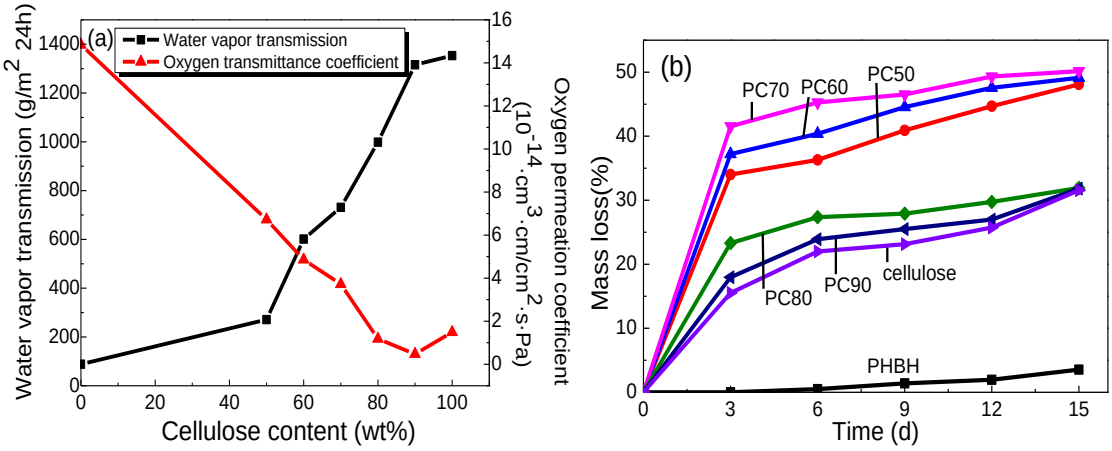

Fig. 5. Water vapor transmission rate and oxygen permeation coefficient curves (a) and mass loss rate curves (b) of PHBH/cellulose composites

Biodegradation

The mass loss rate curves of PHBH, cellulose, and PHBH/cellulose composite films are shown in Fig. 5(b). With increasing cellulose content, the mass loss rate first increased and then decreased. The mass loss rate of neat PHBH film was very low, which was attributed to the hydrophobicity of PHBH making the water molecules and microorganisms difficult to reach, even though the surface of PHBH had more pores and the structure was loose. When the cellulose content increased from 50 wt% to 70 wt%, the mass loss of composite films increased gradually. This was because the hydrophilicity of the composite films was enhanced when the cellulose content was increased, and more water molecules were adsorbed on the surface of the films. Then, the water molecules attacked the ester bonds on the PHBH chain to form carboxyl terminates and terminal hydroxyl groups, promoting the autocatalytic hydrolysis of the ester bonds of PHBH and accelerating the degradation rate of the composite films (Saad and Seliger 2004). When the cellulose content increased from 80 wt% to 100 wt%, the mass loss rate decreased gradually. This result was because fewer PHBH particles were wrapped into cellulose, which was difficult to degrade. The presence of more cellulose led to an orderly and dense arrangement of cellulose macromolecules. Thus, degradation of microorganisms could only start from the surface, reducing the degradation rate of the composite films.

CONCLUSIONS

1. Poly(3-hydroxybutyrate-co-3-hydroxyhexanoate) (PHBH)/cellulose composite films with good mechanical properties, thermal stability, and biodegradability were prepared by the solution casting method.
2. The PHBH/cellulose composite films exhibited a significant improvement in tensile strength compared with neat PHBH and neat cellulose. A substantial increase from 28.5 MPa to 45.9 MPa in tensile strength was observed for PHBH/cellulose

biocomposite films. With increasing cellulose content, the elongation at break of biocomposite films decreased.

3. The thermal stability of the composite films was improved, and the maximum pyrolysis temperature increased from 264 °C to 330 °C.
4. When the cellulose content was 70%, the degradation rate reached its maximum, with a mass loss of 50.2% after 15 d of degradation.
5. The PHBH biocomposites containing high cellulose content have promising potential to be used as a biodegradable material for packaging applications.

ACKNOWLEDGMENTS

This work was financially supported by the National Natural Science Foundation of P. R. China (Nos. 31870564, 31270607).

REFERENCES CITED

Adebajo, M. O., and Frost, R. L. (2004). "Infrared and ^{13}C MAS nuclear magnetic resonance spectroscopic study of acetylation of cotton," *Spectrochim. Acta A* 60(1-2), 449-453. DOI: 10.1016/S1386-1425(03)00249-X

Anderson, S., Zhang, J., and Wolcott, M. P. (2013). "Effect of interfacial modifiers on mechanical and physical properties of the PHB composite with high wood flour content," *J. Polym. Environ.* 21(3), 631-639. DOI: 10.1007/s10924-013-0586-y

ASTM D882-10 (2010). "Standard text method for tensile properties of thin plastic sheeting," ASTM International, West Conshohocken, PA, USA.

Codou, A., Guigo, N., van Berkel, J. G., de Jong, E., and Sbirrazzuoli, N. (2017). "Preparation and crystallization behavior of poly(ethylene 2,5-furandicarboxylate)/ cellulose composites by twin screw extrusion," *Carbohyd. Polym.* 174, 1026-1033. DOI: 10.1016/j.carbpol.2017.07.006

Dasan, Y. K., Bhat, A. H., and Ahmad, F. (2017). "Polymer blend of PLA/PHBV based bionanocomposites reinforced with nanocrystalline cellulose for potential application as packaging material," *Carbohyd. Polym.* 157, 1323-1332. DOI: 10.1016/j.carbpol.2016.11.012

Dong, T., Mori, T., Aoyama, T., and Inoue, Y. (2010). "Rapid crystallization of poly(3-hydroxybutyrate-co-3-hydroxyhexanoate) copolymer accelerated by cyclodextrin-complex as nucleating agent," *Carbohyd. Polym.* 80(2), 387-393. DOI: 10.1016/j.carbpol.2009.11.036

GB/T 1037-1988 (1988). "Test method for water vapor transmission of plastic film and sheet. Cup method," Standardization Administration of China, Beijing, China.

Hosoda, N., Tsujimoto, T., and Uyama, H. (2014). "Green composite of poly(3-hydroxybutyrate-co-3-hydroxyhexanoate) reinforced with porous cellulose," *ACS Sustainable Chem. Eng.* 2(2), 248-253. DOI: 10.1021/sc400290y

Jiang, F., and Hsieh, Y.-L. (2013). "Chemically and mechanically isolated nanocellulose and their self-assembled structures," *Carbohyd. Polym.* 95(1), 32-40. DOI: 10.1016/j.carbpol.2013.02.022

Jie, C., Sun, X., Lu, C., Zhou, Z., Zhang, X., and Yuan, G. (2016). "Water-soluble cellulose acetate from waste cotton fabrics and the aqueous processing of all-cellulose composites," *Carbohyd. Polym.* 149, 60-67. DOI: 10.1016/j.carbpol.2016.04.086

Kynadi, A. S., and Suchithra, T. V. (2017). "Formulation and optimization of a novel media comprising rubber seed oil for PHA production," *Ind. Crop. Prod.* 105, 156-163. DOI: 10.1016/j.indcrop.2017.04.062

Lin, D., Zhao, G.-l., He, B.-h., and Li, X.-f. (2016). "Application of surface acylated nanocrystalline cellulose in polylactic acid based composite membranes," *Modern Food Sci. Technol.* 32(8), 178-182. DOI: 10.13982/j.mfst.1673-9078.2016.8.027

Luo, M., Li, M., Li, Y., Chang, K., Liu, K., Liu, Q., Wang, Y., Lu, Z., Liu, X, and Wang, D. (2017). "In-situ polymerization of PPy/cellulose composite sponge with high elasticity and conductivity for the application of pressure sensor," *Compos. Commun.* 6, 68-72. DOI: 10.1016/j.coco.2017.10.001

Malmir, S., Montero, B., Rico, M., Barral, L., and Bouza, R. (2017). "Morphology, thermal and barrier properties of biodegradable films of poly(3-hydroxybutyrate-co-3-hydroxyvalerate) containing cellulose nanocrystals," *Compos. Part A-Appl. S.* 93, 41-48. DOI: 10.1016/j.compositesa.2016.11.011

Nie, S. X., Zhang, C. Y., Zhang, Q., Zhang, K., Zhang, Y. H., Tao, P., and Wang, S. F. (2018). "Enzymatic and cold alkaline pretreatments of sugarcane bagasse pulp to produce cellulose nanofibrils using a mechanical method," *Ind. Crop. Prod.* 124, 435-441. DOI: 10.1016/ j.indcrop.2018.08.033

Saad, G. -R., and Seliger, H. (2004). "Biodegradable copolymers based on bacterial poly ((R)-3-hydroxybutyrate): Thermal and mechanical properties and biodegradation behaviour," *Polym. Degrad. Stabil.* 83, 101-110. DOI: 10.1016/S0141-3910 (03) 00230-1

Shankar, S., Wang, L.-F., and Rhim, J.-W. (2017). "Preparation and properties of carbohydrate-based composite films incorporated with CuO nanoparticles," *Carbohyd. Polym.* 169, 264-271. DOI: 10.1016/j.carbpol.2017.04.025

Vanitjinda, G., Nimchua, T., and Sukyai, P. (2018). "Effect of xylanase-assisted pretreatment on the properties of cellulose and regenerated cellulose films from sugarcane bagasse," *Int. J. Biol. Macromol.* 122, 503-516. DOI: 10.1016/j.ijbiomac.2018.10.191

Wang, W., Liang, T., Bai, H., Dong, W., and Liu, X. (2018a). "All cellulose composites based on cellulose diacetate and nanofibrillated cellulose prepared by alkali treatment," *Carbohyd. Polym.* 179, 297-304. DOI: 10.1016/j.carbpol.2017.09.098

Wang, W., Xiao, J., Chen, X., Luo, M., Liu, H., and Shao, P. (2018b). "Fabrication and characterization of multilayered kafirin/gelatin film with one-way water barrier property," *Food Hydrocolloid.* 81, 159-168. DOI: 10.1016/j.foodhyd.2018.02.044

Xie, Y., Kohls, D., Noda, I., Schaefer, D. W., and Akpalu, Y. A. (2009). "Poly(3-hydroxybutyrate-co-3-hydroxyhexanoate) nanocomposites with optimal mechanical properties," *Polymer* 50(19), 4656-4670. DOI: 10.1016/j.polymer.2009.07.023

Article submitted: August 31, 2018; Peer review completed: Oct. 29, 2018; Revised version received and accepted: Nov. 29, 2018; Published: December 20, 2018.
DOI: 10.15376/biores.14.1.1219-1228